

# Experimental discovery of the spin-Hall effect in Rashba spin-orbit coupled semiconductor systems

J. Wunderlich,<sup>1\*</sup> B. Kästner,<sup>1,2</sup> J. Sinova,<sup>3</sup> T. Jungwirth<sup>4,5</sup>

<sup>1</sup>Hitachi Cambridge Laboratory, Cambridge CB3 0HE, UK

<sup>2</sup>National Physical Laboratory, Teddington T11 0LW, UK

<sup>3</sup>Department of Physics, Texas A&M University, College Station, TX 77843-4242, USA

<sup>4</sup>Institute of Physics ASCR, Cukrovarnická 10, 162 53 Praha 6, Czech Republic

<sup>5</sup>School of Physics and Astronomy, University of Nottingham, Nottingham NG7 2RD, UK

\*To whom correspondence should be addressed; E-mail: joerg@phy.cam.ac.uk.

**We report the experimental observation of the spin-Hall effect in a two-dimensional (2D) hole system with Rashba spin-orbit coupling. The 2D hole layer is a part of a p-n junction light-emitting diode with a specially designed vertical and planar geometry which allows an angle-resolved polarization detection at opposite edges of the 2D hole system. In equilibrium the angular momenta of the Rashba split heavy hole states lie in the plane of the 2D layer. When an electric field is applied across the hole channel a non zero out-of-plane component of the angular momentum is detected whose sign depends on the sign of the electric field and is opposite for the two edges. Microscopic quantum transport calculations show that the disorder scattering is weak compared to the Rashba coupling in the studied 2D hole system, favoring the intrinsic spin Hall mechanism.**

The Hall effects are among the most recognized families of phenomena in both basic con-

densed matter physics and in applied microelectronics. The ordinary Hall effect, which, e.g., proved the existence of positively charged carriers (holes) in semiconductors and led to the discovery of fractionally charged quasiparticles in the quantum Hall regime, occurs due to the Lorentz force that deflects like-charge carriers towards one edge of the sample creating a voltage transverse to the driving electrical current. The anomalous Hall effect is a response to magnetization in the conducting layer, rather than to an external magnetic field, in which spin-orbit (SO) coupling plays the role of the force that induces the transverse voltage. In this case, like-spin carriers are deflected to one edge and opposite spins to the other edge of the sample which, in a ferromagnetic material, leads to net charge imbalance between the two sides.

In this paper we report the experimental discovery of a new member of the Hall family – the spin-Hall effect (SHE). As suggested in several seminal theoretical works (1–4), the SHE is a direct analog of the anomalous Hall effect but realized in non-magnetic systems. Also reminiscent of the anomalous Hall effect literature is the current intense theoretical discussion upon the origin of the SHE. The extrinsic skew-scattering mechanism (1, 2) is based on asymmetric scattering of spin-up and spin-down electrons from a random impurity potential that includes a SO coupling term. Murakami *et al.* and Sinova *et al.* have recently argued, in contexts of p-doped semiconductors and 2D Rashba coupled systems, that spin-Hall conductivity can be dominated by an intrinsic contribution that follows from distortion of Bloch electrons by the electric field and therefore approaches a disorder independent value in high mobility systems. The robustness of this intrinsic SHE against weak disorder, challenged by several perturbation-theory analytical studies (5–7), has been confirmed by numerical quantum transport calculations based on exact eigenstates of the disordered system and by numerical studies utilizing the Landauer-Buttiker scattering formalisms (8–11). The tremendous interest in the research community generated by the intrinsic SHE follows from the possibilities the effect suggests of inducing and controlling low-dissipative spin-currents in microelectronic devices without applying external

magnetic fields or introducing ferromagnetic elements. Our experimental detection of the SHE is made in a system where the intrinsic effect is only weakly suppressed by disorder and is expected to dominate the spin-Hall response.

Experimentally, the effect has been elusive primarily because in non-magnetic systems the transverse spin-currents do not lead to net charge imbalance across the sample and because a simple “spin-voltmeter” for measuring spin-density gradients does not exist. To maximize the SHE signal and to avoid spurious effects of ohmic contacts in electrical SHE measurements we have fabricated a novel light emitting diode (LED) device which has the following key properties: (i) The SHE is generated in a semiconductor heterojunction 2D hole gas (2DHG) whose ultra-small thickness diminishes the current induced self-field effects and the asymmetric confining potential leads to a strong Rasba SO coupling. (ii) The light is emitted locally from the edges of the 2DHG parallel to the longitudinal current that drives the transverse SHE response. (iii) The circular polarization of the light emitted from the opposite edges of the 2DHG stripe can be measured over the whole range of observation angles between the normal and the plane of the 2DHG. This allows us to detect individual components of the light polarization vector and, hence, the underlying spin orientation of the 2D holes.

The LED was fabricated in a (Al,Ga)As/GaAs double heterojunction structure grown by molecular-beam epitaxy and using modulation donor (Si) and acceptor (Be) doping in the (Al,Ga)As barrier materials. The planar device features were fabricated by optical and electron-beam lithography. The schematics of the semiconductor wafer profile and the numerical simulation of the band-engineered electronic structure are shown in Fig. 1(a). In the as-grown heterostructure, the band-bending leads to a formation of a triangular quantum well in the valence band at the upper (Al,Ga)As/GaAs interface and in the conduction band at the lower interface. The Fermi energy ( $E_F$ ) position results in a purely p-type character of the as-grown semiconductor heterostructure with the conducting 2DHG channel located near the upper

(Al,Ga)As/GaAs interface. The measured 2D hole density is  $p_{2D} = 2 \times 10^{12} \text{ cm}^{-2}$  and the mobility of the 2DHG is  $\mu = 3400 \text{ cm}^2/\text{Vs}$ .

The p-n junction is fabricated by removing the top p-channel from a part of the wafer. In this region the bands are shifted down in energy with respect to  $E_F$ , which leads to the occupation of the lower interface quantum well by electrons and formation of an n-type 2D channel. The diode has a rectifying  $I - V$  characteristic and the onset of the current flow accompanied by electro-luminescence (EL) from the p-n junction step edge occurs at forward bias  $V_{LED} \approx 1.5 \text{ V}$  at temperature  $T = 4.2 \text{ K}$ , which is close to the GaAs band gap, as expected from the band-profile simulations. The LED current is dominated by electrons moving from the n-region to the p-region, while the opposite hole current is negligibly small (12).

In Fig. 1 (b) we plot the measured EL spectra at LED current  $I_{LED} = 85 \mu\text{A}$  and  $T = 4.2\text{K}$ . The energy of peak C coincides with the excitonic recombination energy in bulk GaAs and, consistent with this interpretation, is independent of the LED bias potential. The lower energy peaks A and B are associated with recombination between forward moving 3D electrons in the conduction band and the confined 2D holes. This type II heterojunction recombination is manifested through the peak energies that are below the GaAs band gap and depend on  $I_{LED}$  (12).

To understand the detailed origin of the peaks A and B, which we focus on in this work, we performed microscopic calculations of the 2DHG band-structure based on the 4-band Kohn-Luttinger model (13, 14). As shown in Fig. 1(c), only the lowest 2D subband of the heavy-hole (HH) states is above the  $E_F$ , i.e., is occupied by the 2D holes. At  $k = 0$  the 2D HH and LH subbands are split due to the difference in their out-of-plane masses. The Rashba splitting of the subband occurs due to strong mixing between the HH and light-hole (LH) states induced by the asymmetric confining potential. The typical splitting for the states below the  $E_F$  is  $\sim 5 \text{ meV}$ , similar to the energy splitting of peaks A and B. We associate the peaks A and B with the two

branches of the lowest Rashba SO-split HH subband.

The experimental detection of the SHE in the 2DHG is done by measuring circular polarization (CP) of the emitted light. Due to optical selection rules, a finite CP along a given direction of the propagating light indicates a finite polarization of the carriers that recombine to give such light. It is therefore important to establish first the behavior of the light polarization vector in our structure without applying the p-channel current that drives the spin Hall response. The optical micrograph of the device used for these control experiments is shown in Fig. 2(a). The light detection axis is either close to in-plane perpendicular to the LED current direction (Fig. 2(c,d)) or along the 2DHG plane normal (Fig. 2(e,f)). The key result of these measurements is that at zero magnetic field the in-plane polarization at the two peak positions is finite and has the opposite sign while no perpendicular component of the polarization vector is detected.

To explain this behavior we calculated the expectation values of the components of the total angular momentum  $j = 3/2$  in the two Rashba SO-split HH bands. Note that in the 4-band Kohn-Luttinger representation of the valence band states the total angular momentum and spin operators of the holes are simply related as,  $\mathbf{j} = 3\mathbf{s}$ , and that mixing of the two  $j = 1/2$  valence bands was found to be negligibly small in our 2DHG. Fig. 2(b) shows that the Rashba SO coupling leads to a vanishingly small angular momentum component  $\langle j_z \rangle$  at finite  $\mathbf{k}$ -vectors but to a non-zero in-plane component of  $\mathbf{j}$  oriented perpendicular to the 2D  $\mathbf{k}$ -vector direction. The forward moving electrons that carry the LED current will recombine, through direct optical transitions, with the  $+k_y$  states of the Rashba split HH subbands. The quantum selection rules then lead to a purely in-plane CP of the emitted light with opposite signs corresponding to the two HH branches, consistent with the experimental data at zero magnetic field.

The tunability of the peak A and B polarization vectors by external fields and the ability to detect out-of-plane HH momentum polarizations, which are crucial for the SHE experiment, are demonstrated in the magnetic field dependence of the measured polarization vector. The

cooperative or competing effects of the in-plane field to the Rashba SO coupling are clearly seen in Fig. 2(c) and (d). Depending on the sign of the applied field and on the peak, the in-plane polarization either increase or decreases, changing sign eventually. The asymmetric behavior of the two peaks is not surprising given the asymmetry between the two HH subbands in the absolute values of the SO-induced  $\langle j_x \rangle$  in the  $+k_y$  part of the spectra at zero field (see Fig. 2(b)). By adding a perpendicular Zeeman field, the theoretical expectation values of  $j_z$  become comparable to  $\langle j_x \rangle$  at field strength of  $\sim 1$  T. This and also the opposite signs for the two HH branches is consistent with the out-of-plane circular polarizations of peaks A and B observed in experiment with magnetic fields applied perpendicular to the 2DHG plane (see Fig. 2(e),(f)).

In the SHE, the non-zero expectation value of  $\mathbf{j}$  occurs as a response to external electric rather than magnetic field. To measure this response we drive a current along the p-channel,  $I_p$ , and measure the CP of the light propagating perpendicular to the 2DHG and emanating from the LED at either side of the p-channel. This is a measure of the out-of-plane spin-polarization at the edges of the p-channel since  $\langle j \rangle \propto \langle s \rangle$  for the hole system in the  $j = 3/2$  4-band subspace. The SHE device whose scanning electron micrograph is shown in Fig. 3 (a) was fabricated on the same (Al,Ga)As/GaAs wafer as the device in Fig. 2.

The CP spectra arising from the p-n junction LED on one edge of the p-channel show a flip of the sign when the p-channel current is reversed, confirming that the effect observed is a Hall coefficient. To highlight the effect we plot in Fig. 3 (b) (green line) the difference between the CP spectra for  $+I_p$  and  $-I_p$  when the LED current is send through the upper p-n junction (see LED1 in Fig. 3 (a)). Opposite circular polarizations for opposite  $I_p$  current directions are observed at both peaks A and B. We note that the peak energies are shifted to higher values compared to the spectra in Figs. 1 and 2 due to a larger LED current,  $I_{LED} = 150 \mu\text{A}$ , used in the SHE measurements. On the other hand, neither peak is shifted when the  $I_p$  is reversed since

the drift in the hole distribution due to  $I_p||\hat{x}$  is orthogonal to the 3D electrons drift arising from  $I_{LED}||\hat{y}$  which determines the position of the peaks. For comparison, we show in Fig. 3 (b) (black line) that no perpendicular to 2DHG plane CP was detected in the device of Fig. 2 where  $I_p=0$ . To verify that in the SHE device the spin-polarization is opposite at the two edges of the p-channel we take the difference between the spectra for  $+I_p$  at LED1 and LED2 and obtain a resolution of the same A and B peaks although with a lower efficiency due to asymmetries in the edges at each side, as shown in Fig. 3 (c).

In the remaining paragraphs we discuss the origin of the SHE in our Rashba SO-coupled 2DHG. The intrinsic spin-Hall effect is illustrated schematically in Fig. 3 (e) where the holes at the Fermi surface are displaced by an amount  $|eE\Delta t/\hbar|$  in a time  $\Delta t$  and during this motion they experience a torque imparted by the effective Zeeman field due to the SO coupling. The torque tilts the spins of holes up or down depending on the sign of the  $k_y$ -component of the wavevector. This effect is what is captured in the microscopic calculation of the linear response SHE conductivity in the Kubo formalism which includes a finite quasiparticle lifetime (4, 15–17). A numerical evaluation of the SHE conductivity utilizing the realistic band structure of the 2DHG is shown in Fig. 3 (f) as a function of lifetime-broadening  $\eta = \hbar/\tau$  and 2D hole density. In our structure we are well within the red region which exhibits a spin-Hall conductivity of approximately  $2.5 e/8\pi$ . This is lower than the one obtained assuming the infinitely narrow quantum well approximation and low densities (17) but still considerably larger than the one in n-doped Rashba coupled 2D systems (4).

At the measured mobility of the 2DHG and calculated effective mass of  $0.27m_e$ , the lifetime broadening is estimated at 1.2 meV which is much lower than the Fermi energy measured relative to the top of the HH subbands and the average Rashba splitting. The extrinsic spin-Hall effect arises from the asymmetric scattering from the disorder potential of the different spin species due to the SO coupling. This is illustrated in Fig. 3 (d). The extrinsic mechanism

is expected to dominate in systems where the SO-split bands are not resolved due to the disorder broadening, which is not the case here. A rough estimate (18) of the relative value of the extrinsic and intrinsic SHE conductivities can be obtained by considering each contribution independently;  $|\sigma_{SHE}^{ex}/\sigma_{SHE}^{in}| \sim \alpha(\hbar/m_e c)^2 p_{2D} \sqrt{E_F/\eta}$ , where  $\alpha \sim 10^4$  is the enhancement factor of the Bloch quasiparticles, the Fermi energy is measured from the top of the HH subbands, and the intrinsic SHE conductivity  $\sigma_{SHE}^{in}$  is assumed to be of the order of  $e/8\pi$ . In our system the ratio is much smaller than 1, confirming that the intrinsic mechanism is dominant.

The experimental discovery of the SHE in a Rashba SO coupled system opens new avenues for exploring spin manipulation in non-magnetic semiconductors and its exploitation in low-dissipative electronic devices. Among the next steps in this new research field is to explore experimentally and theoretically the relation between the spin-Hall currents and spin accumulation whose complexity arises from the fact that spins not only precess in the electric field but also relax through various mechanisms. The transmission of the SHE generated polarization from one part to another part of a semiconductor device is another milestone in this scientific endeavour towards the functional SHE based spin-electronics.

## References and Notes

1. M. I. Dyakonov, V. I. Perel, *Sov. Phys. JETP* p. 467 (1971).
2. J. E. Hirsch, *Phys. Rev. Lett.* **83**, 1834 (1999).
3. S. Murakami, N. Nagaosa, and S.-C. Zhang, *Science* **301**, 1248 (2003); cond-mat/0308167.
4. J. Sinova, D. Culcer, Q. Niu, N. A. Sinitsyn, T. Jungwirth, and A.H. MacDonald, *Phys. Rev. Lett.* **92**, 126603 (2004); cond-mat/0307663.
5. J. Inoue, G. E. Bauer, L. W. Molenkamp, *Phys. Rev. B* p. 041303 (2004).



6. E.G. Mishchenko, A.V. Shytov, and B.I. Halperin, cond-mat/0406730 (2004).
7. E. I. Rashba, cond-mat/0409476 (2004).
8. K. Nomura, J. Sinova, T. Jungwirth, Q. Niu, and A. H. MacDonald, cond-mat/0407279 (2004).
9. B.K. Nikolić, L.P. Zârbo, and S. Souma, cond-mat/0408693 (2004).
10. L. Sheng, D. N. Sheng, and C. S. Ting, cond-mat/0409038 (2004).
11. E. M. Hankiewicz, L.W. Molenkamp, T. Jungwirth, and J. Sinova cond-mat/0409334 (2004).
12. B. Kaestner, D. G. Hasko, D. A. Williams, *Jpn. J. Appl. Phys.* **41**, 2513 (2002).
13. R. Winkler, *Phys.Rev.* **B 62**, 4245 (2000).
14. B. Lee, T. Jungwirth, A. MacDonald, *Phys. Rev.* **B 65**, 193311 (2002).
15. J. Schliemann, D. Loss, *Phys. Rev.* **B 69**, 165315 (2004).
16. N. A. Sinitsyn, E. M. Hankiewicz, W. Teizer, J. Sinova, *Phys. Rev.* **B 70**, 081312 (2004).
17. J. Schliemann and D. Loss, cond-mat/0405436 (2004).
18. S. Murakami, N. Nagaosa, S.-C. Zhang, *Science* **301**, 1348 (2003).
19. We thank Allan H. Macdonald and Mohamed N. Khalid for many useful discussions and acknowledge financial support of the Grant Agenct of the Czech Republic.

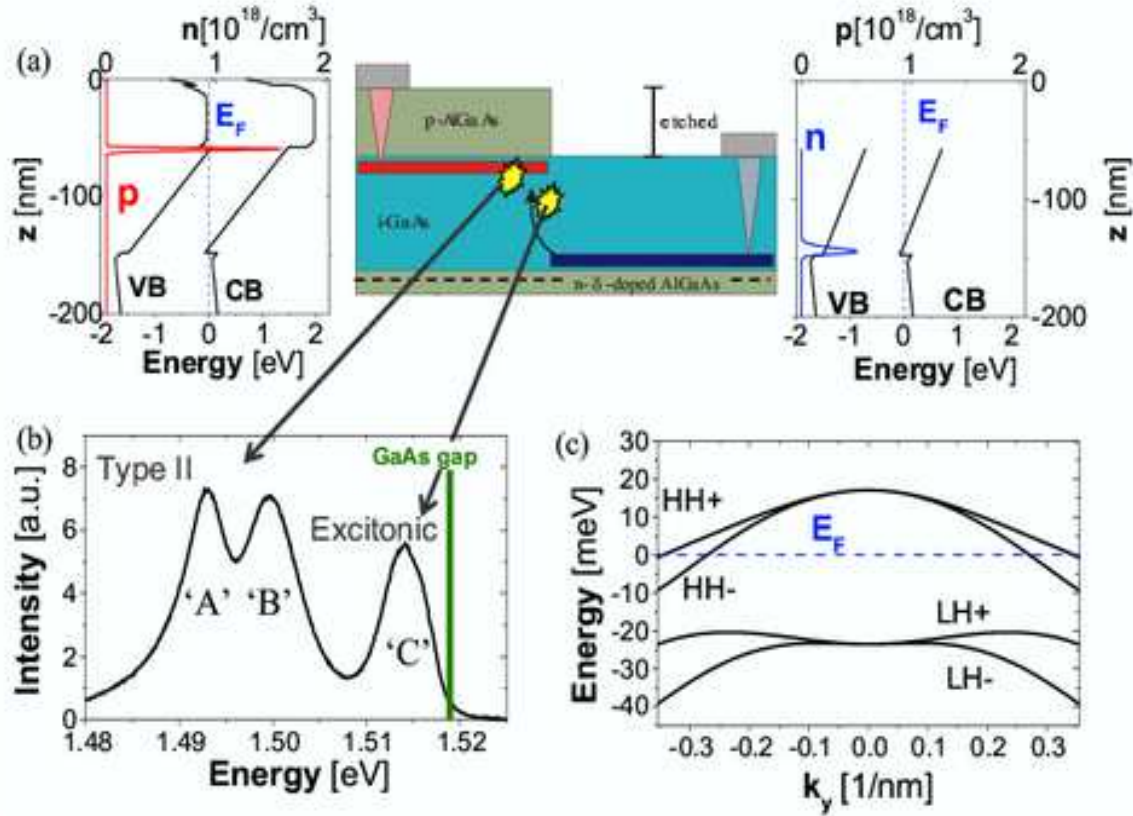


Figure 1: (a) The cross-section of the LED device. The middle schematic diagram shows the n-type 2D channel (dark blue) near the lower (Al,Ga)As/GaAs interface in the etched part of the wafer, the p-type 2D channel (red) below the upper interface in the as-grown part, and the 90 nm thick GaAs layer (light blue) between the two interfaces. The left and right side panels show theoretical simulations of the engineered conduction and valence band profiles in the as-grown and etched regions, respectively. (b) The electro-luminescence spectrum showing the bulk GaAs excitonic recombination peak (C) and the peaks (A,B) corresponding to type II recombination between 3D electron - 2D hole states near the p-n junction step edge. (c) Theoretical energy spectrum of the 2DHG showing the lowest 2D subbands at  $k_x = 0$  of the heavy-hole (HH) and light-hole (LH) valence band states. At  $k = 0$  the 2D HH and LH subbands are split due to the difference in their out-of-plane masses. The splitting at finite  $k$ -vectors of the individual subbands is due to the Rashba SO-coupling induced by the inversion asymmetry of the 2DHG confining potential. The Fermi energy is above the LH subband maximum, i.e., holes are only in the  $\text{HH}^+$  and  $\text{HH}^-$  bands.

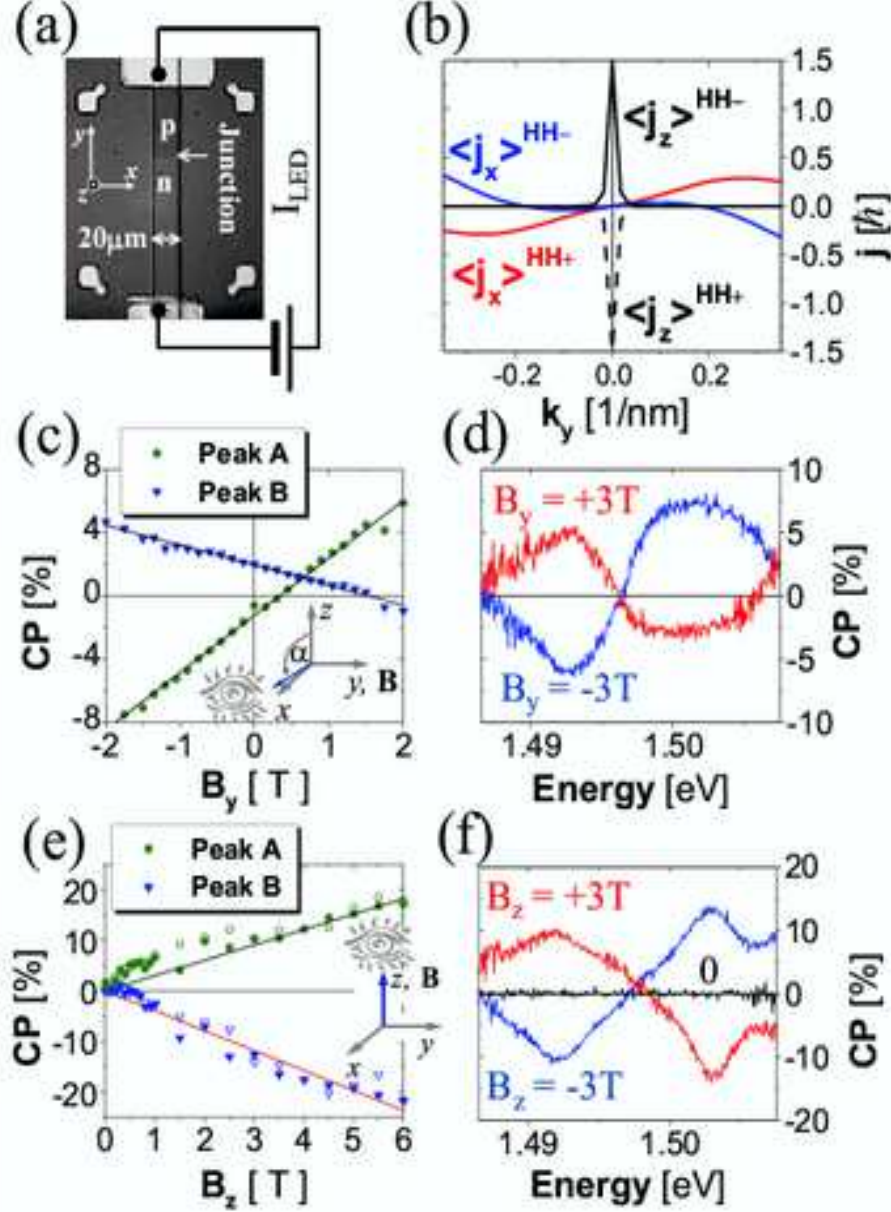


Figure 2: (a) Optical microscopy image of the p-n junction device used in the control experiments with zero SHE driving current along the p-channel. (b) Theoretical expectation values of the  $j_x$ -component and  $j_z$ -component of the total angular momentum plotted as a function of  $k_y$  for the  $HH^+$  and  $HH^-$  subbands.  $\langle j_y \rangle = 0$  for  $k_x = 0$  states consistent with the Rashba SO-coupling mechanism. (c) Circular polarization, defined as the relative difference between intensities of left and right circularly polarized light, plotted as a function of the in-plane magnetic field applied along the y-axis. The observation angle is  $\alpha = 85^\circ$  which is the maximum detection angle allowed in our experimental set-up. The experiment measures, to high accuracy, the x-component of the light polarization vector which is proportional to  $\langle j_x \rangle$ . (d) Spectral plot of the circular polarization near the peaks A and B for  $B_y = \pm 3$  T. (e) Same as (c) for magnetic field and light detection axis along the normal to the 2DHG plane. (f) Same as (d) for  $B_z = +3, 0$ , and  $-3$  T. At zero magnetic field the z-component of the light polarization vector is zero consistent with the theoretical  $\langle j_z \rangle = 0$  at finite  $k$ -vectors.

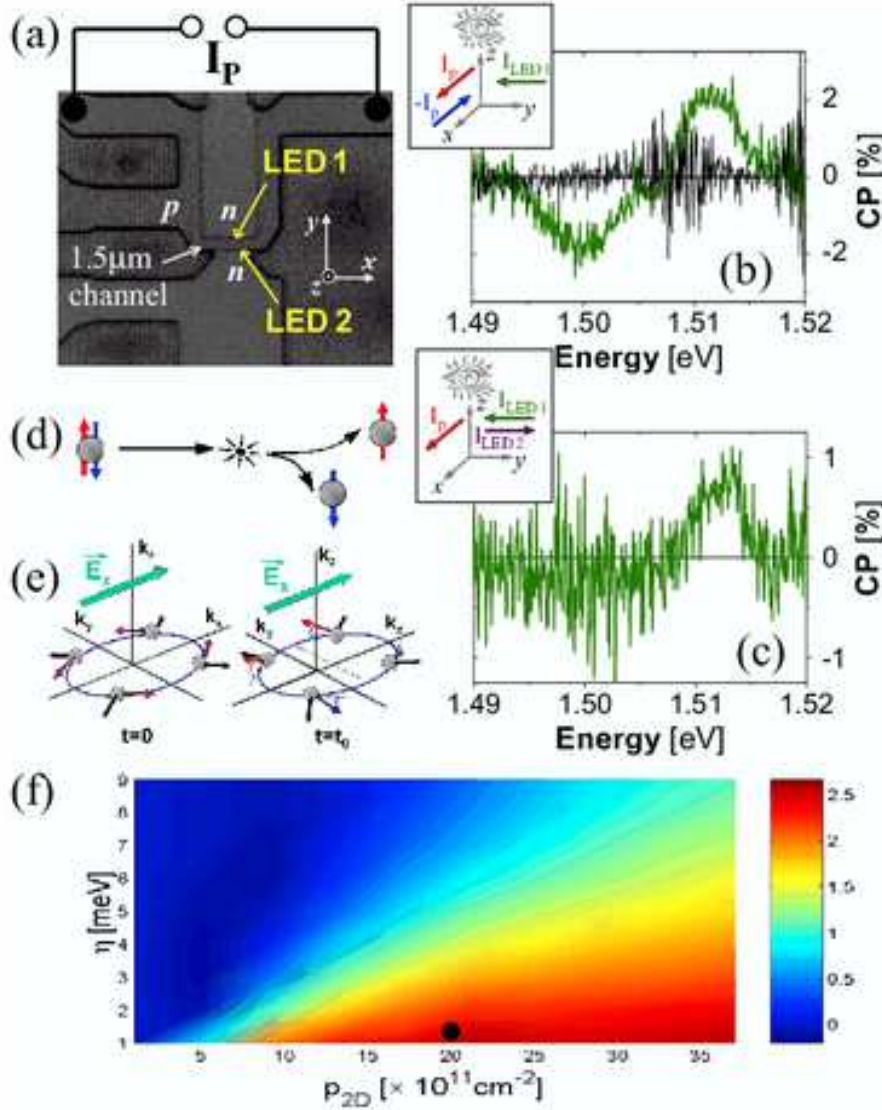


Figure 3: (a) Scanning electron microscopy image of the SHE LED device. The top and bottom n-contacts are used to induce the electro-luminescence at the top and bottom edges of the p-channel, respectively. The current driven along the p-channel drives the SHE response. (b) Difference in the circular polarization at zero observation angle between  $+I_p$  and  $-I_p$  currents in one side of the p-channel (green curve). For comparison we show the perpendicular to 2DHG plane CP in the device of Fig 2 where  $I_p = 0$  (black curve). (c) Difference in the circular polarization between opposite sides of the p-channel observed at zero angle for the p-channel current  $+I_p$ . (d,e) Schematic diagrams of the extrinsic and intrinsic SHE mechanisms (f) Theoretical spin-Hall conductivity in units of  $e/8\pi$  vs. disorder broadening and 2D hole density; sample parameters are indicated by a black dot.